



Guiding Spin Spirals by Local Uniaxial Strain Relief

Pin-Jui Hsu,¹ Aurore Finco,^{1,2} Lorenz Schmidt,¹ André Kubetzka,¹
Kirsten von Bergmann,^{1,*} and Roland Wiesendanger¹

¹*Department of Physics, University of Hamburg, D-20355 Hamburg, Germany*

²*Département de physique, École normale supérieure, 45 rue d'Ulm, 75005 Paris, France*

(Received 22 May 2015; published 5 January 2016)

We report on the influence of uniaxial strain relief on the spin spiral state in the Fe double layer grown on Ir(111). Scanning tunneling microscopy (STM) measurements reveal areas with reconstruction lines resulting from uniaxial strain relief due to the lattice mismatch of Fe and Ir atoms, as well as pseudomorphic strained areas. Magnetic field-dependent spin-polarized STM measurements of the reconstructed Fe double layer reveal cycloidal spin spirals with a period on the nm scale. Globally, the spin spiral wave fronts are guided along symmetry-equivalent $[11\bar{2}]$ crystallographic directions of the fcc(111) substrate. On an atomic scale the spin spiral propagation direction is linked to the $[001]$ direction of the bcc(110)-like Fe, leading to a zigzag shaped wave front. The isotropically strained pseudomorphic areas also exhibit a preferred magnetic periodicity on the nm scale but no long-range order. We find that already for local strain relief with a single set of reconstruction lines a strict guiding of the spin spiral is realized.

DOI: 10.1103/PhysRevLett.116.017201

Noncollinear spin states, such as spin spirals [1] or Skyrmion lattices [2] can form in ultrathin $3d$ transition metal films grown on $5d$ transition metal substrates due to the presence of strong interfacial Dzyaloshinskii-Moriya interaction (DMI) [3,4]. Spin-polarized scanning tunneling microscopy (SP-STM) has proven to be a reliable tool to reveal such complex spin textures [4] and to study their response to external magnetic fields [5] and temperature [6]. For instance, cycloidal [1,5] or conical [7] spin spiral states with unique rotational sense have been discovered in transition metal monolayer (ML), double-layer (DL), as well as mixed bilayer films. Spin spirals in quasi-1D chains as well as Skyrmions have been proposed for information transport in future spintronic devices [8,9]. However, tailoring the fundamental characteristics of such noncollinear spin states, such as their propagation direction, remains an important task in view of their potential application in future spin-based devices.

While the role of the DMI at surfaces and interfaces has already been considered for the stabilization of noncollinear spin textures in ultrathin films [4] and multilayers [10], the influence of strain has remained experimentally unexplored so far. Theoretically, it has been proposed that layer relaxations may significantly modify the magnetic ground state configuration [11,12] and that magnetic phase transition can take place under the application of an in-plane compression [13]. Such strain effects can be expected to occur in heteroepitaxial systems with a sizable lattice mismatch. Several previous experimental SP-STM studies have been performed on epitaxially grown layers of transition metals. While in such systems the magnetic layers are typically strained to adapt to the lattice constant

of the substrate, e.g., Refs. [1,2,5,7,12], it has not yet been possible to extract strain-related effects on the magnetic ground state experimentally. The prime goal of the present study has been to reveal, with atomic-scale spatial resolution, the influence of uniaxial strain relief on a noncollinear spin state stabilized by the DMI.

Here, we report on the discovery of a cycloidal spin spiral state in the Fe DL on Ir(111) and the influence of uniaxial strain relief. As a result of the large lattice mismatch between the Fe DL grown on the fcc Ir(111) substrate, reconstruction lines are formed which can be resolved in constant-current STM images. Magnetic field-dependent SP-STM images reveal the presence of cycloidal spin spirals. The global spiral wave vector follows the reconstruction lines, thereby forming well-ordered spin spiral networks. Locally the spin spiral wave fronts exhibit a zigzag shape, which can be explained by the symmetry of the underlying atom arrangement. In contrast, strained pseudomorphic Fe DL areas also exhibit a spin spiral state, but the period is shorter and the propagation direction is arbitrarily orientated.

Figure 1(a) shows an overview of a sample with about 1.6 atomic layers of Fe grown on an Ir(111) surface at elevated temperatures. While the monolayer (ML) grows pseudomorphic in fcc stacking [12], the double layer (DL) exhibits areas with reconstruction lines (Fe_R) as a result of uniaxial strain relief, as well as pseudomorphic strained patches (Fe_S). As can be seen from a comparison between Figs. 1(b) and 1(c) the appearance of the reconstruction lines is strongly bias dependent [14]. They run perpendicular to close-packed atomic rows of the substrate with a periodicity of about 5.2 nm, and occur in three

rotational domains. From previous studies of epitaxial growth it is known that bcc materials preferentially form a bcc(110)-like interface with a fcc(111) surface [20–22]. Under the assumption that the bottom Fe layer remains pseudomorphic we can model the atomic structure by a uniaxial compression of the top Fe layer by about 5%, resulting in a ratio of 20 Fe atoms of the top layer to 19 Fe atom distances of the bottom layer. We arrive at a structure model for the two Fe layers as shown in Fig. 1(d), which exhibits two mirror-symmetric bcc(110)-like areas (blue rectangles mark the unit cells) separated by lines of fcc- and hcp-like stacking of the top Fe atoms. One type of these hollow site lines [h_2 , cf. Figs. 1(b) and 1(c)] seems to have occasional defects, most likely vacancies. Our experimental data is in agreement with this structure model. However, in a real system we expect small deviations of the atom positions due to relaxation resulting in a small variation of the local strain.

To investigate the magnetic state of the reconstructed Fe DL we employ SP-STM under external magnetic fields [23,24]. Figures 2(a) and 2(b) show constant-current STM

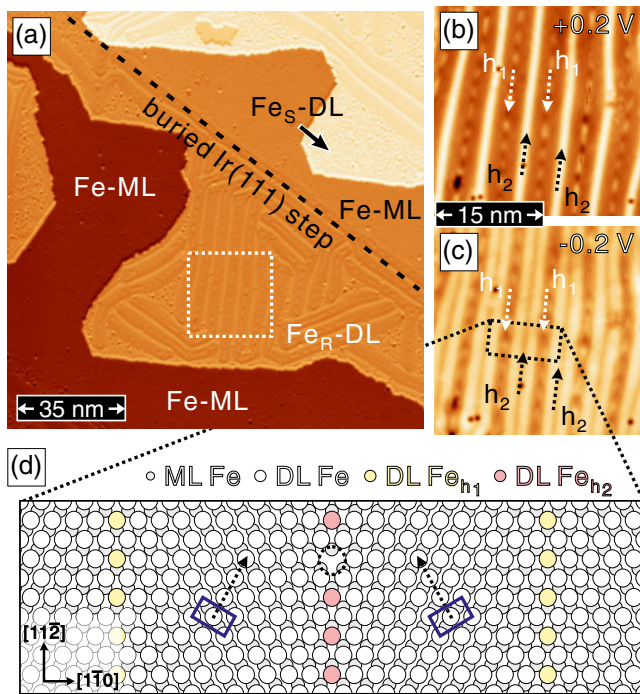


FIG. 1. (a) STM topography of about 1.6 atomic layers of Fe on an Ir(111) surface (measurement parameters: $U = +0.2$ V, $I = 1$ nA, $T = 4.8$ K). The Fe ML grows pseudomorphically. The Fe DL consists of reconstructed (R) and strained (S) areas. (b),(c) Magnified topography images [see box in (a)] of a reconstructed area with periodic reconstruction lines due to uniaxial strain relief taken at $U = +0.2$ and $U = -0.2$ V, respectively. (d) Atomic structure model of the reconstructed Fe DL with a 5% horizontally compressed Fe top layer on a pseudomorphic hexagonal Fe bottom layer; this locally leads to bcc(110)-like areas (blue rectangles) separated by hollow site reconstruction lines (yellow, pink).

images taken at different bias voltages as indicated with all three structural rotational domains. The tip was prepared by controlled collisions with the Fe DL film to have a superparamagnetic cluster at the apex. In our experiment this leads to a time-averaged non-spin-polarized signal for the measurement at zero field, Figs. 2(a) and 2(b); see also the Supplemental Material [14–19]. However, when a magnetic field was applied this tip became magnetically aligned along the direction of the magnetic field. Since the magnetic state of the sample is not influenced by the available external magnetic field (even up to 9T out-of-plane, not shown here), this enables a measurement of

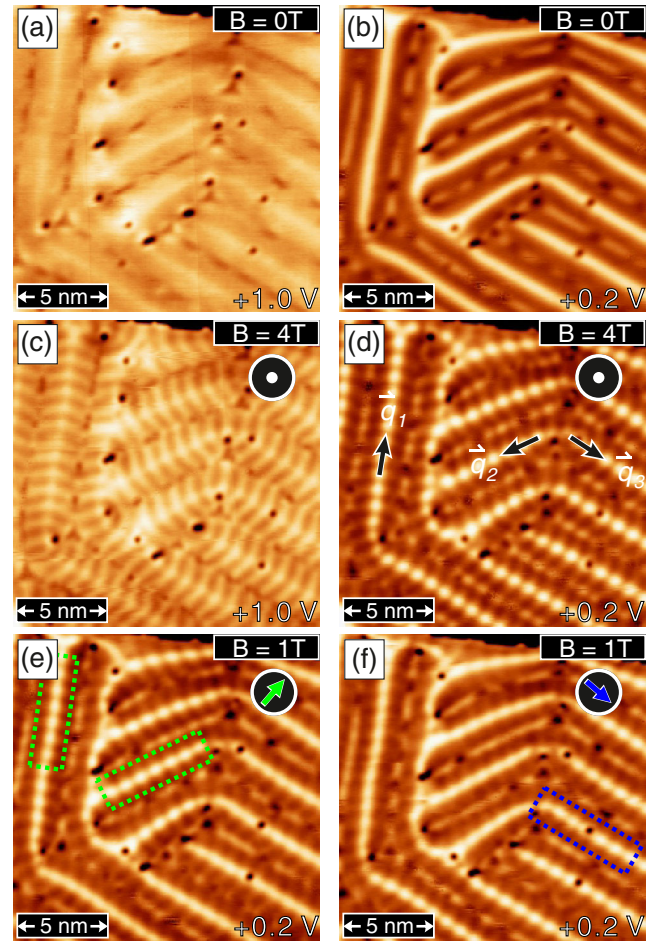


FIG. 2. (a),(b) Spin-averaged topography images of the reconstructed Fe DL with three rotational domains taken at $U = +1.0$ and $U = +0.2$ V, respectively. The typical period of the reconstruction is 4.7 nm, compatible with about 6% strain relief, or 18/17 Fe atoms in the two Fe layers. (c),(d) SP-STM topography images performed at the same location in an out-of-plane magnetic field of 4 T [14]. (e),(f) SP-STM topography images taken in orthogonal in-plane magnetic fields, exhibiting the respective in-plane magnetization component resulting from an alignment of the tip magnetization along the fields. The green and blue empty boxes indicate the maximum magnetic corrugation amplitudes of the different \vec{q} vectors (measurement parameters: $I = 1$ nA, $T = 4.8$ K).

different magnetization components at the identical sample position in our STM setup with vectorial magnetic field [18,25]. The measurements of Figs. 2(c) and 2(d) were performed in an out-of-plane magnetic field and the observed modulations with a period of about 1.6 nm reflect the out-of-plane magnetization components of the sample. The magnetic contrast is found to be strongly bias voltage dependent and it is also slightly different for the electronically inequivalent sites of the top Fe layer, i.e., bcc, hcp, or fcc [14]. The periodic pattern within one rotational domain is indicative of spin spiral order and in Fig. 2(d) the symmetry equivalent propagation directions are labeled with \vec{q}_i individually. It is striking that the \vec{q}_i are strictly parallel to the local orientation of the reconstruction lines, i.e., perpendicular to the direction of uniaxial strain relief.

While with an out-of-plane magnetized tip, Figs. 2(c) and 2(d), the amplitude of the out-of-plane magnetic signal is identical for all three rotational domains, this is not the case for measurements with an in-plane sensitive magnetic tip, as shown for the two orthogonal magnetization directions of the tip in Figs. 2(e) and 2(f). We find that for a tip magnetization m_t perpendicular to \vec{q}_i , the magnetic contrast on the reconstruction lines vanishes [cf. Fig. 2(e) with m_t perpendicular to \vec{q}_3], whereas the magnetic contrast is maximum when m_t is parallel to \vec{q}_i [\vec{q}_3 in Fig. 2(f)]. This leads to the conclusion that the spin spirals are cycloidal, i.e., \vec{q}_i lies in the plane of the spin rotation. According to symmetry arguments this is the spin spiral type typically favored by interface-induced DMI [4,9], and we conclude that the strong DMI found at the interface of Fe ML and Ir(111) [2] also contributes to the observed spin spiral ground state in the reconstructed Fe DL.

In the overview image of Fig. 3(a) with larger rotational domains it becomes apparent that the spin spiral wave fronts are not straight lines but exhibit a zigzag shape. To qualitatively understand the occurrence of this zigzag wave front we have to go back to the structure model of Fig. 1(d): in the areas where the atom arrangement is bcc-like we find lines of atoms along bcc[001], (see dashed arrows). For the Fe DL on Cu(111) [22] and also for the Fe DL on W(110) [18] the spin spiral propagation vector \vec{q} has been found to be parallel to that bcc[001]-like line of atoms. For the latter system two different explanations have been proposed: first, a Monte Carlo study attributed the direction of magnetic domain walls, analogous to spin spiral wave fronts, to Heisenberg exchange interaction in an anisotropic atom environment [26]; second, density functional theory calculations found the direction of the DM vector to be the decisive origin for the direction of \vec{q} [27]. Assuming that also in our Fe DL on Ir(111) \vec{q} couples to the local atom configuration and prefers to be along bcc[001], we immediately arrive at the observed zigzag wave front, see Fig. 3(b): due to the reconstruction, the direction of bcc[001]-atom lines periodically varies [dashed arrows in Fig. 3(b)], meaning that every time a reconstruction line is crossed

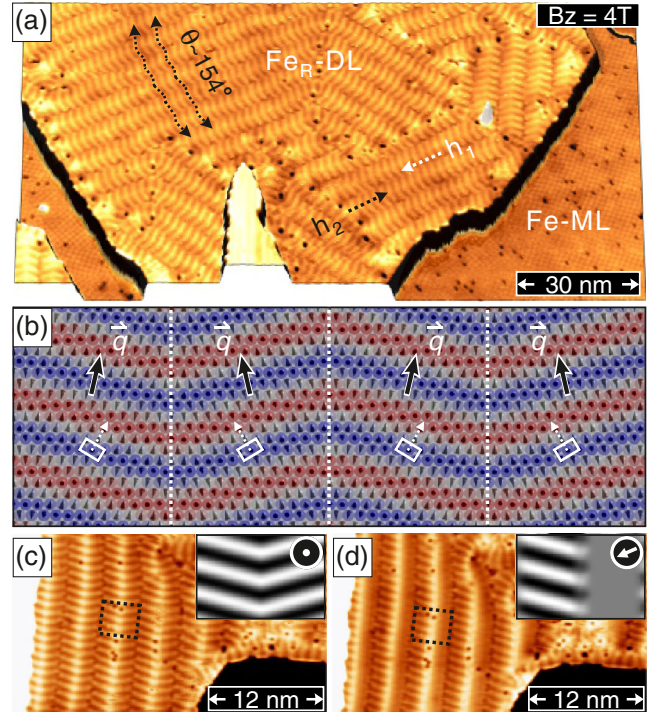


FIG. 3. (a) Overview SP-STM topography image of the spin spiral in the Fe DL and the nanoskyrmion lattice in the Fe ML; the zigzag shape of the spin spiral wave fronts with an angle of $\theta \sim 154^\circ$ is indicated (measurement parameters: $U = +1.0$ V, $I = 1$ nA, $T = 4.8$ K). (b) Sketch of the magnetic state of the reconstructed Fe DL, as deduced from the SP-STM measurements. (c), (d) SP-STM topography images of the zigzag spin spiral measured with an out-of-plane and in-plane spin-sensitive tip, respectively. The corresponding SP-STM simulations are in the insets (measurement parameters: $U = +0.5$ V, $I = 1$ nA, $T = 7.8$ K, $B_z = 2.5$ T).

also the direction of \vec{q} changes. However, a quantitative analysis reveals that the measured zigzag angle is larger than the one expected from the structure model, i.e., about 154° in the measurement versus 117° expected from the structure model with 6% strain relief as in Fig. 3(a). We attribute this to the competition between the coupling of \vec{q} to the atomic lattice and the energy due to kinks in the spin spiral wave front.

To evaluate the local magnetization direction within the zigzag spin spiral we analyze the spin-polarized constant-current images of Figs. 3(c) and 3(d), which are taken at the same location with different tip magnetization directions [14]. From the images we infer that the magnetic signal in Fig. 3(c) represents a dominant out-of-plane component with similar magnetic contrast on all three rotational domains. A close inspection of the zigzag structure of Fig. 3(c) shows that the spin spiral tracks are linked at the position of the bright dislocation line, forming downward pointing arrowheads, whereas they are not strongly correlated across the darker reconstruction lines, i.e., here sometimes the neighboring spin spiral tracks are out of

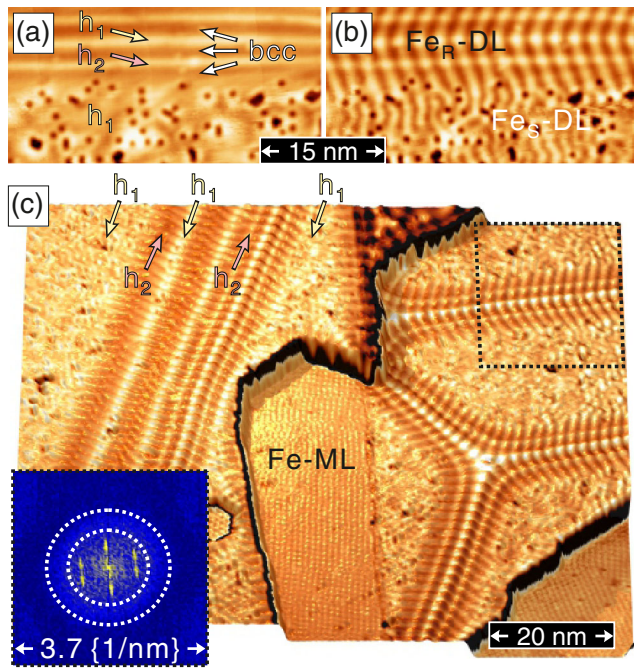


FIG. 4. (a) Spin-averaged topography of the Fe DL on Ir(111) and (b) SP-STM measurement of the same area [14]. Comparison shows the magnetic contribution to the image in (b) (measurement parameters for both: $U = +0.2$ V, $I = 1$ nA, $T = 7.8$ K, $B_z = -1.55$ T). (c) Perspective SP-STM overview topography image. The FFT shown in the inset is taken from the dashed box (measurement parameters: $U = +0.2$ V, $I = 1$ nA, $T = 7.8$ K, $B_z = 0$ T).

phase. In Fig. 3(d) the tip magnetization lies in the plane and for one rotational domain only one bcc-like area of the zigzag spin spiral exhibits magnetic contrast, whereas the other one does not (see dashed box). We conclude that not only are the \vec{q} vectors periodically canted with respect to the dislocation lines, but also the planes of the spin rotation are canted to locally form cycloidal-type spin spirals, as sketched in Fig. 3(b). Simulated SP-STM images with tip magnetization directions as in the experiment are displayed in the insets to Figs. 3(c) and 3(d) for comparison. This means that not only is \vec{q} linked to the strain-induced reconstruction, but also the fine structure of the spin texture is intimately tied to the local atom arrangement.

To identify the magnetic state of the fully strained pseudomorphic Fe DL, spin-averaged and spin-polarized measurements of the same sample area have been performed as presented in Figs. 4(a) and 4(b). Direct comparison reveals that the modulations observed in Fig. 4(b) are of magnetic origin. In the strained Fe DL (bottom) a smaller magnetic periodicity is observed compared to the spin spiral state along the reconstruction line (top). Figure 4(c) shows an overview image of a sample where already isolated reconstruction lines are found to guide the spin spirals perpendicular to the direction of local uniaxial

strain relief. The magnetic state in the interior of the strained Fe DL area appears to be disordered and in order to analyze the periodicity of the magnetic modulations we examine the fast Fourier transform (FFT) of the area in the right upper corner (dashed box). The spots in the FFT originate from the reconstruction lines $h_2 - h_1 - h_2$ and the zigzag spin spiral with a period of about 1.9 nm, whereas the ring (inside the white dashed circles) represents the signal from the strained area. A radial average reveals a peak corresponding to a real space periodicity of about 1.2 nm; i.e., the strain modifies the periodicity of the magnetic state. The ring shape in the FFT is due to the fact that the spin spiral is not propagating along certain directions as expected for a hexagonal surface. Instead, the magnetic state has broken up into many small arbitrarily oriented spin spiral fragments, possibly due to an increased impurity density. This leads to a preferred short-range magnetic periodicity with no long-range order. The implications of these strain-related difference can be nicely seen in the right part of Fig. 4(c), where sets of reconstruction lines strictly guide the spin spirals, not influenced by the strained magnetically isotropic environment.

In summary, the Fe DL on Ir(111) forms a robust spin spiral ground state. The nature of the spin spiral is cycloidal, in line with a significant contribution to the ground state formation by the DMI, which is known to be particularly strong at the interface of an Fe ML and Ir(111). For the strained hexagonal Fe DL the spin spiral propagation direction is found to be arbitrarily oriented and together with small rotational fragments this leads to a spin spiral state with only short-range magnetic order. In contrast to this, already local uniaxial strain relief by incorporation of isolated reconstruction lines leads to a strict guiding of this spin spiral. Strain relief over large areas leads to an extended spin spiral with the global propagation direction along the periodic reconstruction lines. However, locally the propagation direction is very sensitive to the local atomic structure, leading to a zigzag shape of the spin spiral wave fronts. This shows that by introducing uniaxial strain both locally as well as globally the propagation direction of spin spirals can be imposed onto otherwise isotropic magnetic materials. This may become important for epitaxially grown samples such as magnetic multilayers in view of the design of magnetic properties by tailored material strain.

Financial support from the German research foundation (SFB668 and GrK 1286) and the École normale supérieure (Paris) is gratefully acknowledged.

*Corresponding author.

kbergman@physnet.uni-hamburg.de

[1] M. Bode, M. Heide, K. von Bergmann, P. Ferriani, S. Heinze, G. Bihlmayer, A. Kubetzka, O. Pietzsch, S. Blügel, and R. Wiesendanger, *Nature (London)* **447**, 190 (2007).

- [2] S. Heinze, K. von Bergmann, M. Menzel, J. Brede, A. Kubetzka, R. Wiesendanger, G. Bihlmayer, and S. Blügel, *Nat. Phys.* **7**, 713 (2011).
- [3] A. Fert and P.M. Levy, *Phys. Rev. Lett.* **44**, 1538 (1980).
- [4] K. von Bergmann, A. Kubetzka, O. Pietzsch, and R. Wiesendanger, *J. Phys. Condens. Matter* **26**, 394002 (2014).
- [5] N. Romming, C. Hanneken, M. Menzel, J.E. Bickel, B. Wolter, K. von Bergmann, A. Kubetzka, and R. Wiesendanger, *Science* **341**, 636 (2013).
- [6] A. Sonntag, J. Hermenau, S. Krause, and R. Wiesendanger, *Phys. Rev. Lett.* **113**, 077202 (2014).
- [7] Y. Yoshida, S. Schröder, P. Ferriani, D. Serrate, A. Kubetzka, K. von Bergmann, S. Heinze, and R. Wiesendanger, *Phys. Rev. Lett.* **108**, 087205 (2012).
- [8] M. Menzel, Y. Mokrousov, R. Wieser, J.E. Bickel, E. Vedmedenko, S. Blügel, S. Heinze, K. von Bergmann, A. Kubetzka, and R. Wiesendanger, *Phys. Rev. Lett.* **108**, 197204 (2012).
- [9] A. Fert, V. Cros, and J. Sampaio, *Nat. Nanotechnol.* **8**, 152 (2013).
- [10] B. Dupé, G. Bihlmayer, S. Blügel, and S. Heinze, arXiv:1503.08098.
- [11] A. Deák, L. Szunyogh, and B. Ujfalussy, *Phys. Rev. B* **84**, 224413 (2011).
- [12] K. von Bergmann, S. Heinze, M. Bode, E. Y. Vedmedenko, G. Bihlmayer, S. Blügel, and R. Wiesendanger, *Phys. Rev. Lett.* **96**, 167203 (2006).
- [13] T. Shimada, J. Okuno, and T. Kitamura, *Phys. Rev. B* **85**, 134440 (2012).
- [14] See the Supplemental Material at <http://link.aps.org/supplemental/10.1103/PhysRevLett.116.017201>, which includes Refs. [15–19].
- [15] S. Loth, K. von Bergmann, M. Ternes, A. F. Otte, C. P. Lutz, and A. J. Heinrich, *Nat. Phys.* **6**, 340 (2010).
- [16] S. Loth, C. P. Lutz, and A. J. Heinrich, *New J. Phys.* **12**, 125021 (2010).
- [17] A. A. Khjetoorians, B. Baxevanis, C. Hübner, T. Shlenk, S. Krause, T. O. Wehling, S. Lounis, A. Lichtenstein, D. Pfannkuche, J. Wiebe, and R. Wiesendanger, *Science* **339**, 55 (2013).
- [18] S. Meckler, N. Mikuszeit, A. Preßler, E. Y. Vedmedenko, O. Pietzsch, and R. Wiesendanger, *Phys. Rev. Lett.* **103**, 157201 (2009).
- [19] F. Meier, L. Zhou, J. Wiebe, and R. Wiesendanger, *Science* **320**, 82 (2008).
- [20] E. Bauer and J. H. van der Merwe, *Phys. Rev. B* **33**, 3657 (1986).
- [21] B. An, L. Zhang, S. Fukuyama, and K. Yokogawa, *Phys. Rev. B* **79**, 085406 (2009).
- [22] S.-H. Phark, J. A. Fischer, M. Corbetta, D. Sander, K. Nakamura, and J. Kirschner, *Nat. Commun.* **5**, 5183 (2014).
- [23] M. Bode, *Rep. Prog. Phys.* **66**, 523 (2003).
- [24] R. Wiesendanger, *Rev. Mod. Phys.* **81**, 1495 (2009).
- [25] S. Meckler, M. Gyamfi, O. Pietzsch, and R. Wiesendanger, *Rev. Sci. Instrum.* **80**, 023708 (2009).
- [26] E. Y. Vedmedenko, A. Kubetzka, K. von Bergmann, O. Pietzsch, M. Bode, J. Kirschner, H. P. Oepen, and R. Wiesendanger, *Phys. Rev. Lett.* **92**, 077207 (2004).
- [27] M. Heide, G. Bihlmayer, and S. Blügel, *Phys. Rev. B* **78**, 140403(R) (2008).